

# Periodicity Manifestations in the Non-Locally Coupled Maps

Tokuzo Shimada and Shou Tsukada

Department of Physics, School of Science and Technology, Meiji University  
 Higashi-Mita 1-1-1, Kawasaki, Kanagawa 214-8571, Japan  
 (May 20, 2019)

We study how periodicity manifestations recently found in the turbulent globally coupled maps depend on the global feature of the couplings. We examine three non-locally coupled map models. In the first two, the all-to-all interaction is maintained but the coupling decreases with distance in a power and an exponential law. In the third, the interaction is uniform but cut off sharply. We find that, in all three and in dimension  $D = 1; 2; 3$ , periodicity manifests universally from turbulence when the same suppression of the local mean field fluctuation is achieved by the non-local averaging.

05.45.+b, 05.90.+m, 87.10.+e

The globally coupled map lattice (GCM L) is one of the basic models of complex systems with interacting chaotic elements. The simplest GCM L consists of  $N$  identical logistic maps with uniform couplings via their mean field  $h_t$ . It has only two parameters, the non-linearity  $a$  of element map and the coupling  $\mu$  of the averaging interaction. Yet it exhibits a rich variety of phases under the balance between the randomness and the coherence [1] and provides us with a simple testing ground of basic features of wide variety of coupled random elements such as the Josephson junction array, vortex dynamics, multimode lasers as well as biological networks. In particular, in its 'turbulent regime' | the region of high non-linearity and very weak coupling | the system at large  $N$  exhibits intriguing properties in evolution.

Firstly, the maps are under unfailing weak coherence even if the parameters are so chosen that no visible synchronization of maps occurs [2]. As a result the mean square deviation (MSD) of the time series of mean field  $h_t$  is sizably enhanced from the value predicted by the law of large numbers ( $\overline{h^2} / 1=N$ ), while the  $h_t$  distribution is Gaussian following the central limit theorem [2]. This was called as a hidden coherence and triggered much scrutiny [3{5]. Furthermore, it has been recently found that the periodic windows of the element map systematically foliate and produce various periodicity manifestations (PM's) [6{9]. Therefore, GCM L in the turbulent regime is a system which sensitively mirrors the periodic windows with the background hidden coherence. The amazing fact that even at very weak coupling the system easily form periodic cluster attractors may have important consequences in a complex system of coupled chaotic elements, especially in the activity of the brain.

In this Letter we study to what extent the PM's depend on the all to all uniform coupling feature of GCM L. We will show that they occur universally in three non-locally coupled map models and their strength can be predicted by a simple estimation of the fluctuation of local mean fields around the overall mean field.

The PM's are organized by the maps by synchronization when the parameters  $a; \mu$  are in a balance that allows a reduction of the high  $N$ -dimensional dynamics to that of the element logistic map in a periodic window at non-linearity  $b$ . The balance defines foliation curves on the  $(a; \mu)$  plane and all GCM L on the curves are universally governed by the window dynamics. The most prominent PM's are induced by the period three window [6]. If GCM L is on the foliation curves of the  $p3$  window, the maps organize themselves into almost equally populated three clusters, which oscillate mutually in period three |  $p3c3$  maximally symmetric cluster attractor (MSCA) [7]. With slightly higher  $\mu$  at the same  $a$ , that is, on the foliation curves from the intermittent region, the maps organize themselves in  $p3c2$  cluster attractor. The  $p3$  attractors are formed at any reduction factor  $r$  ( $r = a - 1$ ). Generally, for a small reduction ( $r > 0.95$ ), maps form  $p = c$  MSCA and  $p > c$  clusters respectively along the curves of period  $p$  window and in the nearby higher  $\mu$ . In MSCA, the MSD of the mean field fluctuation is minimized due to the high population symmetry and all observed MSCA's are linearly stable [7]. Contrarily, in  $p > c$  states, the MSD turns out extremely high due to missing clusters to fill the orbits. For a large reduction ( $r < 0.95$ ), the clusters are no longer formed but their remnants induce the same structure in the MSD | a valley and peak respectively along the curves of a window and in the nearby higher  $\mu$ . We use below the MSD curve as a representation of PM's.

Non-locally coupled map models. | The GCM L on the lattice is

$$x_p(t+1) = (1 - \mu) f(x_p(t)) + \mu h_t; P \geq 2 \tag{1}$$

with the mean field  $h_t = (1/N) \sum_{Q=2}^P f(x_Q(t))$  and  $f(x) = 1 - ax^2$ . This is a two step process; the independent mapping followed by an interaction via the mean field  $h_t$  with an overall coupling  $\mu$ . By adding (1) over  $P$  we find a

relation  $\frac{1}{N} \sum_{P \in \mathcal{P}} x_P^0 = \frac{1}{N} \sum_{P \in \mathcal{P}} f(x_P)$  | the mean field is kept invariant in the interaction. All the non-local models we consider below respect this invariance rule.

A power law model: POW. | As an extension of GCM L let us consider a model

$$x_P^0 = (1 - \mu) f(x_P) + \mu h_P;$$

$$h_P = c^{(1)} f(x_P) + d^{(1)} \sum_{Q \in \mathcal{P}} \frac{1}{|Q|} f(x_Q); \quad (2)$$

where each map couples to other maps via a local mean field  $h_P$ . The  $\mathcal{P}$  is a set of maps at an equal distance from a site  $P$ . For simple analytic estimates below, we approximate it by a set of points on the boundary of a  $(2 + 1)^D$  square (cube) for  $D = 2(3)$ . The number of maps in  $\mathcal{P}$ ,  $n$ , is then  $2; 8; 24^2 + 2$  respectively for  $D = 1; 2; 3$ . We impose the periodic boundary condition and the maximum 'radius' of  $\mathcal{P}$  is  $(N^{1=D} - 1)/2$ . As a requisite the weights for a local mean field  $h_P$  must add to one. This constrains the coefficients  $c^{(1)}$  and  $d^{(1)}$  as

$$c^{(1)} + d^{(1)} S^{(1)} = 1; \text{ with } S^{(1)} = \sum_{n=1}^{\infty} \frac{1}{|Q|} n = \dots; \quad (3)$$

Under this constraint, one obtains with a simple arithmetic both the above invariance rule and a further important relation  $\frac{1}{N} \sum_{P \in \mathcal{P}} h_P = h$  | the average of the local mean fields is nothing but the mean field of the whole system.

Let us make (2) into a model which interpolates the GCM L and the nearest neighbor CML. In order to match with GCM L at  $\mu = 0$ , the coefficient must be  $c^{(0)} = d^{(0)} = 1/N$ . In order to match with the nearest neighbor CML at  $\mu = 1$ , the coefficient must be  $c^{(1)} = d^{(1)} = 1/(n+1)$ .

$$x_P^0 = f(x_P) + \frac{\mu}{n+1} \sum_{Q \in \mathcal{P}} f(x_Q) - n_1 f(x_P)^A; \quad (4)$$

at  $\mu = 1$ , the coefficients must be  $c^{(1)} = d^{(1)} = 1/(n+1)$ . In both limits,  $c = d$ . Therefore, we set  $c^{(1)} = d^{(1)}$  for all  $\mu$  as the simplest interpolation. Normalizing the couplings by (3), we obtain a one parameter extension of GCM L, POW, with  $h_P$  given by

$$\frac{1}{1 + S^{(1)}} \sum_{Q \in \mathcal{P}} f(x_Q) + \frac{\mu}{1 + S^{(1)}} \sum_{Q \in \mathcal{P}} \frac{1}{|Q|} f(x_Q)^A; \quad (5)$$

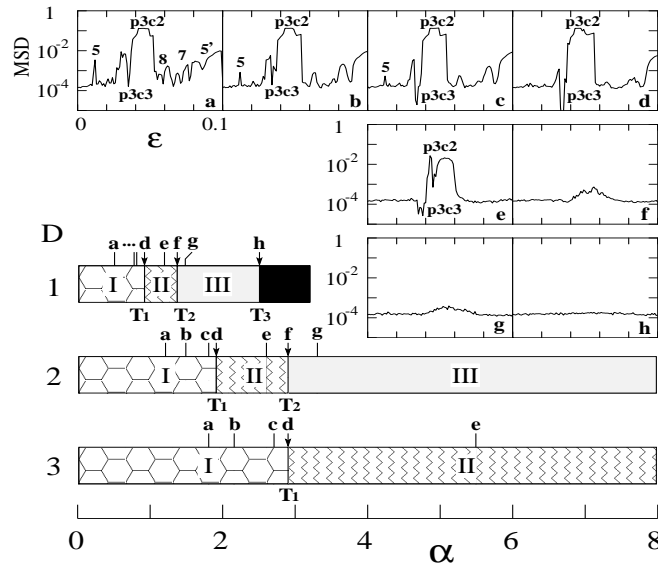


FIG. 1. The bar chart for the PM's in POW with  $a = 1:90$  and the MSD curves at the eight marking points (a-h). I: full PM's, II: only the  $p = 3$  PM's, III: only the hidden coherence.

As shown in Fig. 1 PM's in POW diminish with the increase of  $\epsilon$ . We choose eight marking points (a-h) and in the insets we display corresponding MSD curves. By the strength of PM's the interval may be divided into three regions. (I) One can observe all PM's that occur in GCM L. From the GCM L limit ( $\epsilon = 0$ ) up to the point a, the full strength PM's are produced. The relevant dominant windows are marked on the MSD curve at a, which agrees precisely with the curve in GCM L [7]. From a to d, the peak valley structures, except for that due to p3 clusters, gradually diminish. The peak due to p5 window starts diminishing at a and it becomes half-height at b. At c all the sub-dominant peak-valley structures vanish, and even the p5 peak vanishes at d. (II) The region of p3 PM's only. It starts from d and the p3c2 peak disappears at e. At f, only a broad MSD peak is seen in the MSD curve. (III) Essentially the region of the hidden coherence. Only broad MSD peak can be seen around the foliation zone of the p3 window. At the start of III and near the top of the peak, the correlator of maps decreases exponentially in time in a p3 motion. At g, the broad MSD enhancement becomes half-height and the correlator fails to sense the periodicity everywhere. At h, the MSD enhancement disappears. The transition points  $T_1, T_2, T_3$  between the regions are d, f, h respectively. As we see in the bar chart, the variation of PM's occurs most quickly in  $D = 1$  and it is prolonged in higher dimensions. We note that  $T_1 = 0.9; 1.9; 2.9$ , approximately in the ratios 1:2:3 for  $D = 1; 2; 3$  respectively. An exponentially decaying coupling model:  $\text{EXP}_{\epsilon_0}$ . Similarly, we obtain a model with  $h_p$  given by

$$\frac{1}{1 + S^{(\epsilon_0)}} \exp\left(\sum_{p=1}^D w_p f(x_p)\right) + \sum_{q=2}^D w_q f(x_q)^A; \quad (6)$$

where  $w_p = \exp(-\epsilon_0 p)$  is the exponentially decaying coupling and  $S^{(\epsilon_0)} = \sum_{p=1}^D w_p$ . This reduces to GCM L at  $\epsilon_0 \rightarrow 1$  and the nearest neighbor CML at  $\epsilon_0 \rightarrow 0$ . The PM's diminish with decreasing  $\epsilon_0$  via the same process as above.

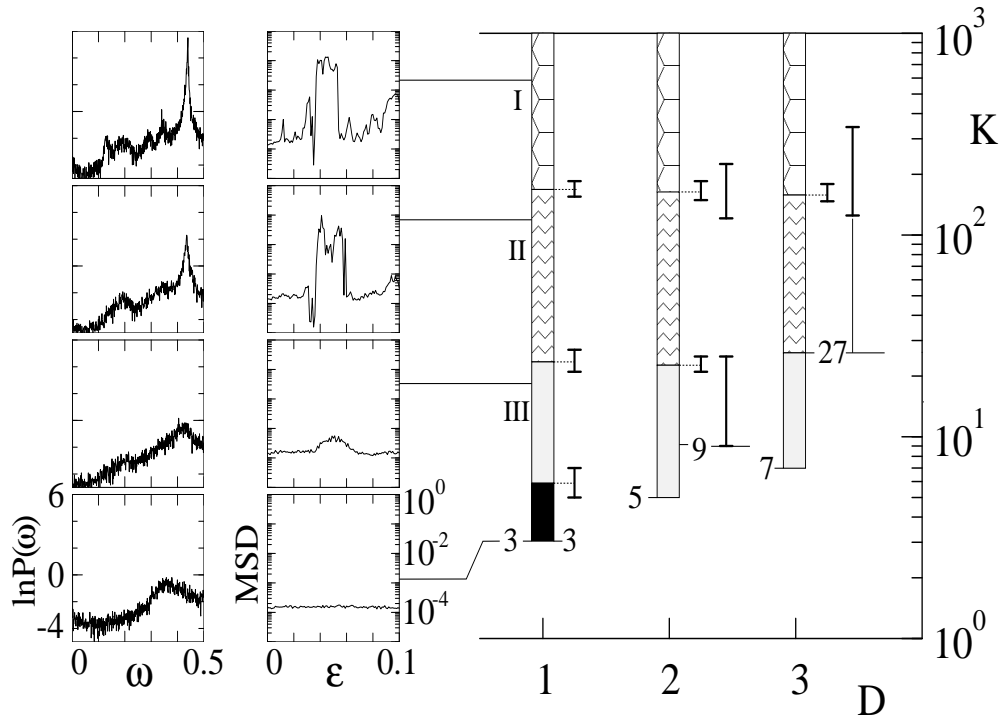


FIG. 2. Right: Bar chart of PM's in CML at  $a = 1:90$ . I: full PM's, II: only the  $p = 3$  PM's, III: only the hidden coherence. The error bars compare the ambiguities in determining the transition points by two types of neighborhood. Center: The MSD curves at the pointed positions. Left: Power spectrum of the mean field at  $(a; \epsilon) = (1.99; 0.10)$  in  $D = 1$ .

A coupled maps with an interaction range  $\epsilon$ : CML. Above two models maintain all-to-all coupling feature of GCM L. Let us now consider a non-local CML with  $h_p$  given by

$$\frac{1}{K} \sum_{P \in \mathcal{Q}} f(\mathbf{x}_P) + \sum_{Q \in \mathcal{P}} f(\mathbf{x}_Q) \quad (7)$$

Here  $K = (2 + 1)^D$  is the number of maps within a range  $\Delta$ . We find that the PM's diminish with decreasing  $\Delta$ , again via the same patterns of MSD curves. Furthermore, we find that remarkably the same PM's occur irrespective to the dimensions if the neighborhood encloses the same number of maps. For instance, the range at  $T_1$  is  $77.92; 5.6; 2.3$  in  $D = 1; 2; 3$  respectively, but the number of maps  $K$  within is  $155.185, 121.169, 125.343$  in  $D = 1; 2; 3$ . The large error in  $D = 3$  comes from the large-step increase of  $K$  with  $\Delta$ . Thus we determine the marking points in CML by a reduced neighborhood; a set of lattice points  $\mathcal{Q}$  around  $P$  with  $\sum_{i=1}^D (\Delta_i)^2 \leq \Delta^2$ .

In Fig. 2 we show the three regions by a bar chart in terms of  $K$ . We find the bars in  $D = 1; 2; 3$  agree each other well. CML was used in an analysis of hidden coherence from the view of beat of mean field [3]. The Fourier power spectrum of  $h_t$  is shown also in Fig. 2. Interestingly, the Fourier peaks due to the beat become outstanding in accord with the onset of PM's. The universality of PM's in non-local models. The difference between GCM and other non-local models is only in the interaction step. In GCM, the maps contract uniformly to  $h$  by a factor  $1 - \epsilon$ , while in others a map  $f(\mathbf{x}_P)$  is contracted to the local mean field  $h_P$  which distributes around the overall system mean field  $h$ . Therefore, when the variance of  $h_P - h$  is large, some distortion of map configuration must unavoidably be introduced in the interaction step. Contrarily, when the variance is small, such a distortion will be avoided and the non-local system may evolve just in the same way with GCM. In CML,  $h_P$  is an equal weight average of  $K$  quasi-random variables. Therefore, the variance of  $h_P$  is suppressed the more for the larger  $K$  and the suppression factor  $F$  may be simply estimated as  $F = 1/K$  by LLN. This estimate is crude; it ignores the hidden coherence and assumes a single  $F$  for various PM's. However, the observation of the same PM's at common  $K$  in CML strongly supports this. Thus, let us propose a working hypothesis that PM's occur universally in all non-local models when the variance of  $h_P$  is the same and see if it works in POW and EXP<sub>0</sub> as well, estimating the suppression factor  $F$  in them using the same independent random number approximation. For  $F$  in POW, we obtain

$$F_D^{(\cdot)} = \frac{1}{(1 + S_D^{(\cdot)})^2} \left( 1 + \sum_{i=1}^D \frac{n_i}{2} \right) \quad (8)$$

taking into account the distance-dependent weights for the contribution of maps to  $h_P$ . The leading  $N$  estimates for  $F_D^{(\cdot)}$  are tabulated in Table. I. We find in particular  $F \sim \log N = 4N$  at  $\Delta = 1; 2; 1; 3 = 2$  for  $D = 1; 2; 3$  respectively. This gives a prediction that the PM's would be universal among POW <sub>$D=1$</sub> , POW <sub>$D=2$</sub>  and POW <sub>$D=3$</sub> . This is indeed the case; the full strength PM's, the same with those in GCM, are realized in all the three. Similarly, the  $F_D^{(0)}$  in EXP<sub>0</sub> may be obtained by substituting  $S_D^{(0)}$  and  $w_{i,0}^2$  to  $S_D^{(\cdot)}$  and  $1 = 2$  respectively.

In Fig. 3 we compare POW (EXP<sub>0</sub>) with CML in the right (left). The inset illustrates the case of the transition point  $T_1$  (d) in  $D = 1$  as an example. The curve is  $F$  for POW in (8). The measured  $F$  at  $T_1$  gives the vertical band taking account for the ambiguity in judging the MSD curve pattern. Hence, the crossing of the curve and the vertical band gives the estimate of  $F$  in POW at its  $T_1$  in  $D = 1$ . On the other hand,  $F$  in CML is simply estimated by  $1/K$  universally over  $D$  as shown in Fig. 2. The  $F$  at  $T_1$  of CML gives the horizontal band, again counting for the ambiguity and averaged over  $D$ . Thus, the vertical axis is used for both  $F$ 's, that in POW and that in CML. If both models share exactly the same  $F$  at  $T_1$ , the curve will pass through the crossing junction of the horizontal and vertical bands. In this example, the curve crosses the vertical band slightly above the junction and the estimated  $F$  are  $(9.1) \cdot 10^{-3}$  and  $(6.05) \cdot 10^{-3}$  in POW and CML respectively. Or, one can predict the  $F$  at  $T_1$  in POW from  $K$  at  $T_1$  in CML using the  $F$  curve of POW. The prediction is  $0.84 \pm 0.04$  to be compared with the measured  $0.90 \pm 0.03$ . In the overall comparison, only the junctions are shown by error-bars. The limits of  $F$  are  $1 = 3^D$  at  $\Delta \rightarrow 1$  (0! 0) | CML limit and  $1 = N$  at  $\Delta \rightarrow 0$  (0! 1) | GCM limit. We find that the hypothesis remarkably works with respect to all the marking points and in  $D = 1; 2; 3$ .

TABLE I. The leading  $N$  estimate of the  $F$  in POW.

$D$	$\Delta = 0$	$\frac{1}{2}$	1	$\frac{3}{2}$	2	$\frac{5}{2}$	3	$\frac{7}{2}$	1
1	$1=N$	$\ln N = 4N$	$2=12 \ln^2 N$	$(3)=2^2 \left(\frac{3}{2}\right)$					$\frac{1}{3}$
2	$1=N$	$9=8N$	$\ln N = 4N$	$2=96 \frac{1}{N}$	$(3)=2 \ln^2 N$	$(4)=8^2 \left(\frac{3}{2}\right)$			$\frac{1}{9}$
3	$1=N$	$25=24N$	$4=3N$	$\ln N = 4N$	$2=36N^{\frac{2}{3}}$	$(3)=48N^{\frac{1}{3}}$	$4=240 \ln^2 N$	$(5)=24^2 \left(\frac{3}{2}\right)$	$\frac{1}{27}$

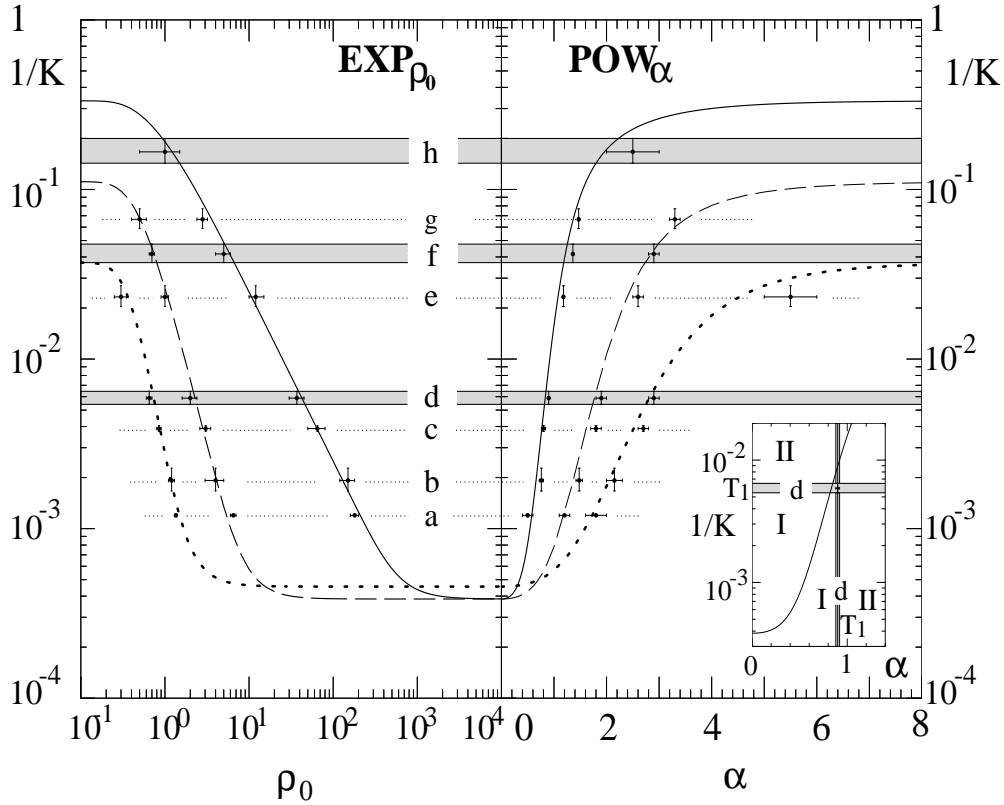


FIG. 3. The comparison between POW and CML (right) and EXP<sub>ρ<sub>0</sub></sub> and CML (left) with respect to eight marked changes (a-h) of the PM's. For  $D = 1; 2; 3$  respectively the  $F_D$  is shown by the solid, dashed, and dotted curves and  $N = 51^2; 51^2; 13^3$ . The inset illustrates the method for the case of  $d(T_1)$  in  $D = 1$ .

A few remarks are in order. (i) The curves in POW agree approximately with each other after a scale transformation  $1:1=2:1=3$  in up to  $F_D = 2 \cdot 10^2$ . This extends the rule obtained by the leading  $N$  calculation. The same strength PM's occur up to the marking point e if  $\alpha$  is in the ratio of the system dimensionality, just like the universal PM's at the same  $K$  in CML. (ii) The horizontal bands exhibit three transition points observed in CML using refined neighborhood. In other models with the coarse neighborhood, the  $T_3$  is missing in  $D = 2$  and both  $T_2$  and  $T_3$  are missing in  $D = 3$ . (See Fig. 1 for POW). The curves of  $F$  explain the difference succinctly; they are constrained by the limiting values  $1=3^D$  so they can pass through only the lowest two (one) bands in  $D = 2(3)$ . We have numerically checked that the missing transition points are retrieved in both POW and EXP<sub>ρ<sub>0</sub></sub> with the refined neighbors. (iii) Contrary to CML, the other two models maintain all to all interaction and  $F$  in them depends on the system size  $N$ . Let us discuss the case of POW. As the leading  $N$  estimate in Table I shows,  $F$  vanishes at the thermodynamical limit if  $1; 2; 3$  in  $D = 1; 2; 3$  respectively, while for the larger  $\alpha$  it approaches a constant from above. Now, we have already chosen  $N > 10^3$ , since it is necessary for the PM's (except for p3) to occur even in GCM L. Thus the marking points a and b are already deep in region I and insensitive to a further increase of  $N$ . The points c to h are also insensitive because of the saturation of  $F$  by a constant. Hence the only place to check the finite size effect is the region near the  $T_1$  and we have verified it ( $F / 1 = \log^2 N$ ). For instance,  $T_1$  in  $D = 2$  POW with  $N = 51^2$  is at  $\alpha = 1.7$  and by replacing  $N$  by  $10^5$  the PM's become into stronger ones at point c in I just as predicted. (iv) Our hypothesis assumes that there is a single  $F$  common to all PM's at different  $\alpha$ . We have verified this by measuring the MSD surface of  $\rho_p$  over the  $N; \alpha$  plane; it has no dependence on  $\alpha$  except for a small hump at p3 region and its dependence on  $N$  is just as predicted by (8).

In conclusion we have studied to what extent the periodicity manifestations recently found in the turbulent GCM L depend on the all to all uniform coupling feature of it. We examined three models, POW, EXP<sub>ρ<sub>0</sub></sub> and CML; all interpolate GCM L and the nearest neighbor CML but in different paths. We have found that periodicity manifests

universally in them, irrespective of the difference in construction and the dimension of the system, once the fluctuation of the local mean field around the overall mean field is the same. Even the finite size effect is under control in our approach.

One of the authors (T.S.) especially thanks Wolfgang Ochs for encouragement and reading the manuscript, and Max-Planck Institut für Physik, München for the warm hospitality, where this work is completed. Our thanks also go to Mario Cosenza for communication and Kengo Kikuchi for collaborating with us at the early stage of this work.

---

- [1] K. Kaneko, Phys. Rev. Lett. 63, 219 (1989).
- [2] K. Kaneko, Phys. Rev. Lett. 65, 1391 (1990).
- [3] S. Sinha, D. Biswas, M. Azam, and S. V. Lawande, Phys. Rev. A 46, 3193 (1992).
- [4] A. S. Pikovsky and J. Kurths, Phys. Rev. Lett. 72, 1644 (1994).
- [5] K. Kaneko, Physica D 55, 368 (1992); D 86, 158 (1995).
- [6] T. Shimada, Tech. Rep. IEICE, NLP 97-159, 71 (1998); T. Shimada, Mem. Inst. Sci. Tech., Meiji Univ., 37, 1-60 (1998).
- [7] T. Shimada and K. Kikuchi, Phys. Rev. E 62, 3489 (2000).
- [8] A. P. Parravano and M. G. Cosenza, Int. J. Bifurcation Chaos 9, 2331 (1999)
- [9] T. Shibata and K. Kaneko, Physica D 124, 177 (1998).